Article

Not peer-reviewed version

Synthesis and Anticancer Evaluation of Some Glycine Conjugated Hybrid Compounds Containing Coumarin, Thiophene and Quinazoline Moieties

Nedime Çalışkan , Emre Menteşe , Fatih Yılmaz * , Muhammed Süleyman İlhan , Mustafa Emirik

Posted Date: 20 August 2025

doi: 10.20944/preprints202508.1398.v1

Keywords: quinazoline; coumarin; thiophene; glycine; prostate cancer (PC-3); breast cancer (MCF-7)

 doi:10.20944/preprints202508.1398.v1

Article

Synthesis and Anticancer Evaluation of Some Glycine Conjugated Hybrid Compounds Containing Coumarin, Thiophene and Quinazoline Moieties

Nedime Çalışkan [1], Emre Menteşe [1], Fatih Yılmaz [2]*, Muhammed Süleyman İlhan [3] and Mustafa Emirik [1]

[1] Department of Chemistry, Faculty of Art and Sciences, Recep Tayyip Erdogan University, 53100 Rize, Turkey

[2] Vocational School of Technical Sciences, Department of Chemistry and Chemical Process Technology, Recep Tayyip Erdogan University, 53100, Rize, Turkey

[3] Department of Biology, Faculty of Engineering and Natural Sciences, Manisa Celal Bayar University, 45140 Manisa, Turkey

* Correspondence: fyilmaz@erdogan.edu.tr

Abstract

Background/Objectives: Cancer is one of the leading causes of death worldwide, so that 10 million people died from cancer worldwide in 2020. Among them, prostate and breast cancer are the most frequently diagnosed cancer in the world. **Methods**: Notably, compound **9f** displayed the highest activity against both Prostate cancer (PC-3) and Breast cancer (MCF-7) cell lines. It was seen that substitution on the coumarin ring had a positive effect on anticancer activity (exept chlorine substitution on 6th position of coumarin), while it had a negative effect on the selectivity index (the ratio of IC50 calculated for healthy and cancer cells). **Conclusions**: The findings are consistent with the results obtained in the Molecular Docking results. Molecular docking studies were performed to investigate the binding affinities of the synthesized compounds towards kinesin-associated motor protein EG5, Human Ribonucleotide Reductase and Human Topoisomerase II, confirming their potent in vitro cytotoxicity against cancer cell lines. In accordance with the findings of experimental studies, compound 9f demonstrated the optimal docking binding scores.

Keywords: quinazoline; coumarin; thiophene; glycine; prostate cancer (PC-3); breast cancer (MCF-7)

1. Introduction

Cancer is one of the leading causes of death worldwide, so that approximately 19.3 million new cases were detected and 10 million people died from cancer worldwide in 2020. According to the world health organization (WHO) and International Agency for Research on Cancer (IARC), cancer cases are expected to reach 28 million by 2040 in the world. This represents an increase of approximately 50% compared to 2020. At the same time, the number of people dying from cancer is expected to increase in a similar way. Also, cancer is the second reason of death worldwide. Therefore, scientists developed novel compounds which have anticancer activities, and significant numbers of them were approved by the Food and Drug Administration (FDA) for treatment of cancer. However, drug resistance and undesirable side effects are key factors limiting the effectiveness of current chemotherapy regimens. To overcome these challenges, there is a need for the development of new anticancer agents that can enhance potency and minimize the side effects [1–3].

Prostate cancer is one of the most diagnosed malignancies and the second largest risk of male mortality after lung cancer in worldwide [4,5]. After the development of cancer in the prostate, cancerous cells can spread to the lungs, pancreas, stomach and bones through angiogenesis.

 doi:10.20944/preprints202508.1398.v1

Angiogenesis is one of the reasons for the development of many diseases such as cancer [6]. It is an important mechanism that tumors use to grow and spread. Cancerous cells can promote angiogenesis to secure a blood supply that supports their growth and allows them to survive, especially as they increase in size [7–9].

Breast cancer is a cancer type which starts in the breast cells. If it is not controlled, the tumor cells can spread throughout the body and be fatal. There were 2.3 million new cases of breast cancer worldwide in 2022. It has resulted in 670 thousand of deaths among women. It can be seen in every woman at any age after puberty. In 2023, approximately one in eight women (approximately 13 %) faced with breast cancer in their lives [10]. The death rate of breast cancer was unchanged between 1930s and 1970s. However, survival rates were increased in the 1990s with early detection and effective drug treatments [11].

The development of effective anticancer compounds aims to overcome some challenges associated with existing treatments, such as severe toxicity and drug resistance [12,13]. Molecular hybridization technique is a classical medicinal chemistry approach for obtaining new bioactive compounds through the combination of different bioactive fragments creating a new hybrid entity endowed with enhanced affinity and potency compared to parent compounds. Also, previous studies have shown that molecular hybridization could be a promising drug design strategy for cancer therapy [14].

Coumarin (2*H*-1-benzopyran-2-one) was first isolated from Tonka bean (Dipteryx odorata) of the Fabaceae family in 1820 [15]. Coumarin derivatives are found as secondary metabolites in many plant species, most commonly in the families of Rutaceae, Apiaceae, Fabaceae and Asteraceae [16]. They can be isolated as novobiocin and aflatoxin from some microbial sources. Approximately 80% of used anticancer drugs are natural compounds [17]. Many researchers have extensively investigated the various mechanisms of coumarin-based anticancer agents including molecular hybridizations [18]. In the search for new anticancer drugs, natural products are always an important source. Many coumarin derivatives obtained from natural products show important anticancer activity [19–22] Moreover, the concept of molecular hybridization can provide efficient results in the treatment with coumarin moiety, as it may lead to the production of new anticancer drugs with lower toxicity, improved specificity, and increased efficacy [23]. In **Figure 1.**, some coumarin derivatives, which are possess anticancer activity, were shown.

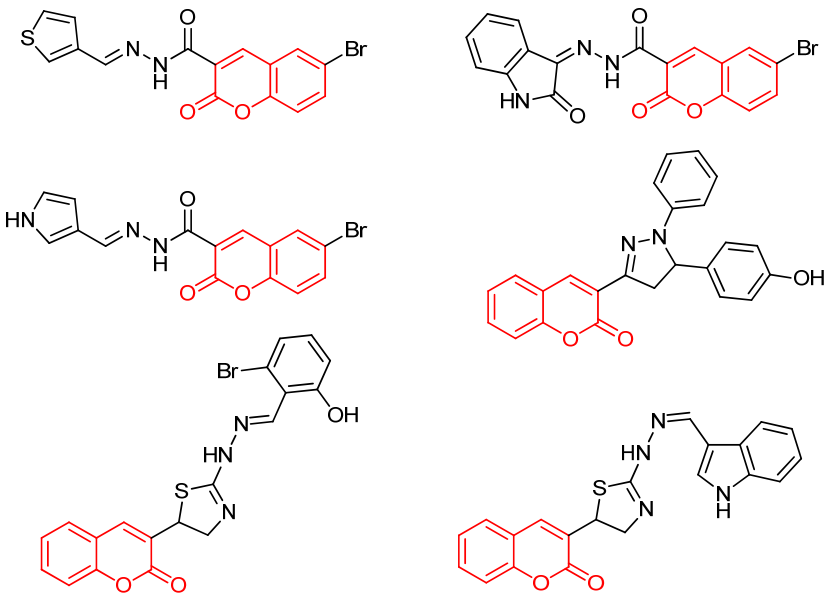

Figure 1. Some anticancer active comarin derivatives.

 doi:10.20944/preprints202508.1398.v1

Quinazoline molecules have been identified as a preferred group of multi-acting therapeutic agents within the pharmaceutical and biological domains. The ease with which it can be prepared, in addition to its diverse pharmacological activities, has led to its significant importance among the various therapeutic agents available. The fundamental approach to the development of novel agents with anticancer activity involves the placement of different substituents at the 4, 6, and 7-positions of the quinazoline system [24,25]. According to literature studies, many quinazoline derivatives have been found to have anti-cancer activity due to their high selectivity and low toxicity [26] (**Figure 2**.).

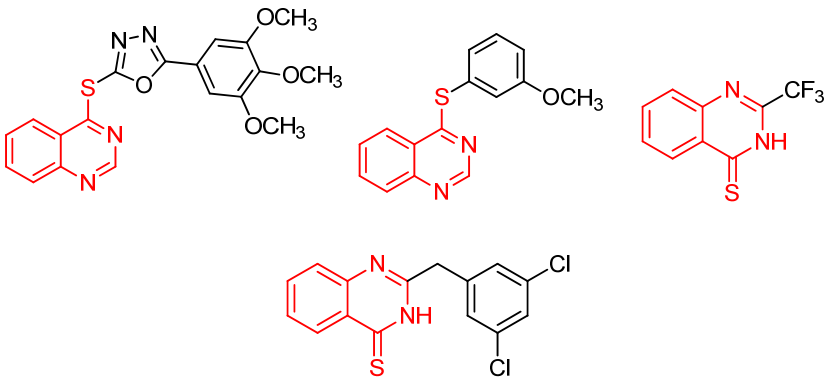

Figure 2. Some anticancer active quinazoline derivatives.

Amino acids are among the most significant molecules in nature, given their role as building blocks of proteins and as intermediates in metabolism [27]. Amino acid molecules bind together to form proteins. The configuration of these proteins is determined by the types of amino acids that they contain, as well as the order in which these amino acids are arranged. the human body contains twenty amino acids, which combine in various ways to form more than 40,000 proteins [28]. Amino acids have been shown to possess special physiological functions, including biocompatibility and cell affinity. These functions render them the most fundamental substances of the biological system. Interaction and selectivity against tumor cells can be increased or decreased through amino acid modification [29]. Amino acids have become interesting molecules to be used in cancer therapy, aiming to reduce the need for genotoxic agents [30]. As demonstrated in literature, amino acid conjugated compounds have the potential to act as chemotherapeutic agents. In addition, amino acid conjugation has been shown to increase antitumor activity in hybrid compounds [31,32] . In **Figure 3.**, some amino acid conjugated anticancer active compounds were shown.

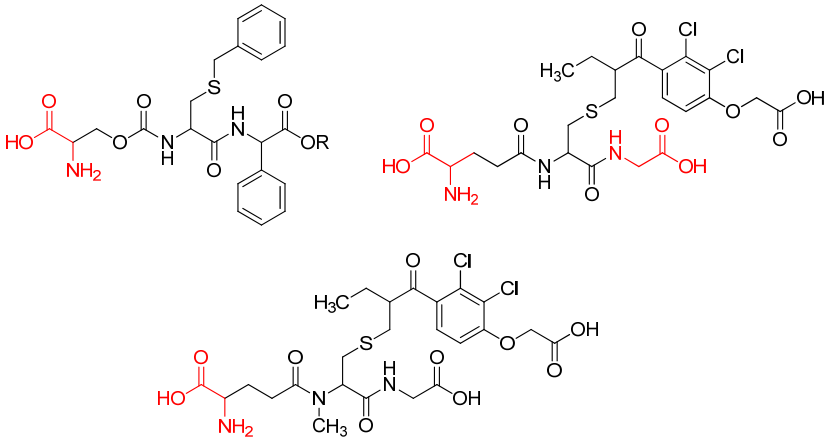

Figure 3. Some anticancer active aminoacid conjugated compounds.

 doi:10.20944/preprints202508.1398.v1

Considering our experience in design and synthesis of novel hybrid molecules [33–40], we focused on the synthesis of novel bioactive molecules containing promising hybrids such as coumarin and quinazoline moieties with the hope of novel anticancer agents which are more active and have less side effects. The results of our literature research show that there are limited studies on the design, synthesis and anticancer evaluation of quinazoline and coumarin containing hybrids. The main purpose / aim of the present work is to synthesize novel hybrid compounds containing quinazoline, thiophene and coumarin cycles, which are found as bioactive compounds in our previous works [33,36,37,41] and determine their anti-cancer properties on Prostate cancer (PC-3) and Breast cancer (MCF-7) cell lines. Interestingly, the findings of the present study demonstrated that substitution on the coumarin ring enhanced anticancer activity, yet concomitantly diminished the selectivity index value. Also, the substitution at 8th position of coumarin resulted in a greater increase in activity than the substitution at 5th position. The findings presented here align with the results obtained from the molecular docking studies.

2. Result and Discussion

2.1. Chemistry

The synthetic routes for preparing target hybrid molecules were carried out in three steps. In the first step, firstly, ethyl 2-(thiophen-2-yl)acetamide hydrochloride (**1**) was prepared as described in literature[42]. Secondly, the 2-aminothiobenzamide was reacted with compound **1** to obtain 2-(thiophen-3-ylmethyl)quinazoline-4(3*H*)-thione (**2**). Then, compound **2** was treated with ethyl bromoacetate to obtain ethyl {[2-(thiophen-2-ylmethyl)quinazolin-4-yl]sulfanyl}acetate (**3**). Lastly, compound **3** was reacted with hydrazine monohydrate to obtain 2-{[2-(thiophen-2-ylmethyl)quinazolin-4-yl]sulfanyl}acetohydrazide (**4)**, which is the first intermediate for the target hybrid compounds (**Scheme 1.**).

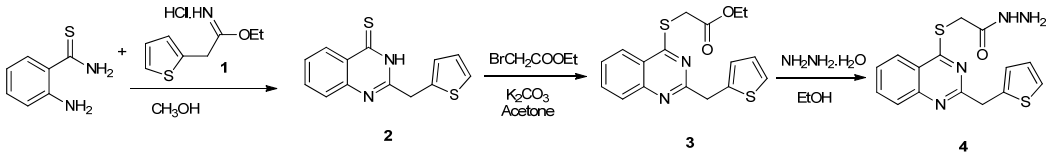

Scheme 1. Synthetic route for compound **4.**

In the second step, firstly, compounds **5a-f** and **6 a-f** were obtained according to our previous studies[33]**.** Then, compounds **6a-f** were reacted with glycine to obtain compounds **7a-f**. Then, compounds **7a-f** were reacted with 1*H*-benzotriazole in dichloromethane to obtain glycine conjugated coumarin benzotriazole compounds **8a-f**, which are the second intermediate for target compounds (**Scheme 2.**).

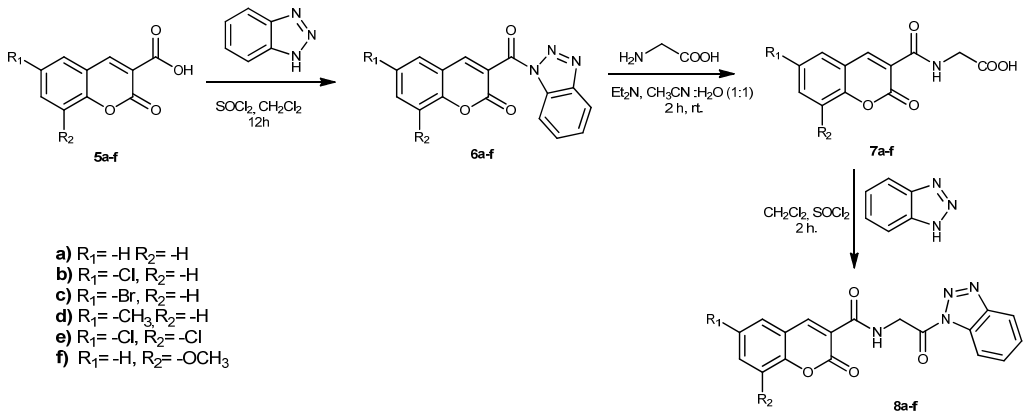

 doi:10.20944/preprints202508.1398.v1

Scheme 2. Synthetic route for compound **8a-f.**

In the last step, compounds **7a-f** were reacted with compound **3** in dimethyl sulfoxide to obtain glycine conjugated hybrid compounds containing quinazolinone, thiophene and coumarin moieties.

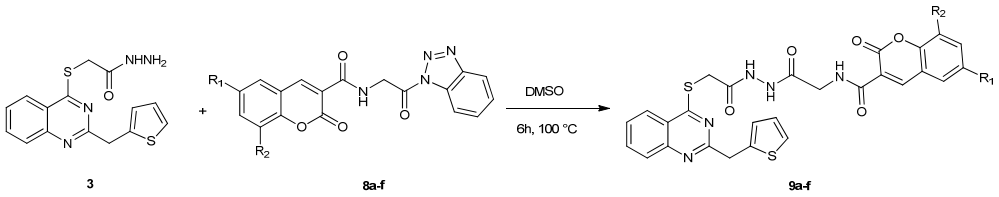

a: R_1= H, R_2= H, **b:** R_1= Cl, R_2= H, **c:** R_1= Br, R_2= H, **d:** R_1= CH_3,R_2= H, **e:** R_1= Cl, R_2= Cl, **f:** R_1= H, R_2= OCH_3

Scheme 3. Synthetic route for compound **9a-f.**

Spectral analyses of target compounds are suitable for the proposed structures. Infrared (IR) spectra of compounds **9a-f** gave NH signals between 3300 and 3100 cm^{-1}, C=O signals between 1750-1610 cm^{-1} and C=N signal at about 1560 cm^{-1}. ^{1}H NMR spectra of these compounds showed three NH signals between 11.80 and 9.20 ppm. Coumarin C_4-H was shown at about 8.90 ppm in ^{1}H NMR spectra of these compounds. Three CH_2 signals were found at about 4.50, 4.10 and 4.00 ppm, which belong to SCH_2, NCH_2 and CH_2 protons, respectively. ^{13}C NMR data of these compounds showed suitable signals with the proposed structures. C=N signal belonging to quinazolinone C_4 carbon atom was shown at about 170 ppm. Three C=O signals were shown between 170.00-157.00 ppm. The other aromatic signals were shown in suitable range and number. When the mass spectra of these compounds were examined, the signals originating from the ^{79}Br and ^{81}Br isotopes found in compound **9b** and the ^{35}Cl and ^{37}Cl isotopes found in compounds **9c** and **9e** were observed in suitable proportions and in accordance with the [M+H]+, [M+Na]+ and [M+K]+ signals. In addition, all compounds gave suitable elemental analysis results indicating the calculated ones.

2.2. Anticancer Activity Study

The CC_{50} values of the target compounds against Prostate cancer (PC-3), Breast cancer (MCF-7), and Human embryonic kidney (HEK 293) cell lines are shown in Table 1. The CC_{50} values were determined in the range of 8.7 ± 2.4-197.6 ± 1.5 µg/L for HEK-293 human healthy embryonic kidney cell line, 14.7 ± 1.4-85.5 ± 1.1 µg/L for Prostate cancer (PC-3), and 16.5 ± 1.2- 104.9 ± 0.9 µg/L for Breast cancer (MCF 7). Some of the synthesized compounds were found to be more active than Cisplatin. Among the synthesized compounds, the compound that showed the best results in terms of toxic effects on human healthy embryonic kidney cell lines was compound **9f**, the compounds that showed the best anticancer activity on PC-3 on human prostate cancer cells were compounds **9f, 9e, 9d, 9c, 9a** and **9b**, while the compounds that were determined to be more active than cisplatin against the breast cancer cell line were compounds **9f, 9e, 9c, 9d, 9a** and **9b**.

Table 1. The anticancer activity and selectivity index (SI) value of synthesized compounds against Prostate cancer (PC-3), Breast cancer (MCF 7), and Human embryonic kidney (HEK 293) cell lines.

CC_{50} (citotoxitity 50: µg/L); SI (selectivity index)					
Comp. no.	**Prostate cancer (PC-3)**	**SI**	**Breast cancer (MCF-7)**	**SI**	**Human embryonic kidney (HEK-293)**
9a	61.3 ± 2.6	3.22	80.7 ± 1.1	2.45	197.6 ± 1.5
9b	85.5 ± 1.1	1.57	104.9 ± 0.9	1.29	134.6 ± 1.6
9c	47.7 ± 0.3	2.51	71.2 ± 0.2	1.68	119.9 ± 2.1
9d	43.0 ± 0.9	2.14	74.3 ± 1.4	1.24	91.9 ± 1.4
9e	34.6 ± 2.2	1.98	46.1 ± 1.4	1.49	68.8 ± 0.8
9f	14.7 ± 1.4	0.59	16.5 ± 1.2	0.53	8.7 ± 2.4

 doi:10.20944/preprints202508.1398.v1

Cisplatin	24.1 ± 0.4	0.85	22.1 ± 1.0	0.93	20.6 ± 2.4

Conventional chemotherapy drugs have been employed in the treatment of cancer for a considerable period; however, they have been associated with significant challenges and deleterious side effects on normal cells. While these drugs are effective in targeting rapidly dividing cancer cells, there is also an unfortunate consequence of destroying healthy cells. It is important to note that the non-specific targeting of traditional chemotherapy drugs can affect both cancer cells and normal cells, which may reduce the effectiveness of treatment and increase the risk of side effects. Another challenge that has the potential to reduce the effectiveness of treatment is the development of drug resistance in cancer cells. The objective of drug development for cancer treatment is therefore to selectively target cancer cells while sparing healthy cells, thereby reducing the impact on normal tissues. In this study, HEK-293 cells were utilized to investigate the cytotoxic effects of the synthesized compounds on normal cells. In contrast to cisplatin, all compounds (with the exception of **9f**) exhibited higher CC50 values in HEK-293 cells compared to cancer cells. This finding suggests that these products are less toxic to normal cells, yet retain their efficacy against cancer cells. In order to assess the cancer cell-specific effects of the synthesized compounds, the selectivity indices (SI) of the compounds were calculated by dividing the CC50 values for normal cells by the CC50 values for cancer cells. Within the domain of anticancer activity, an elevated selectivity index signifies a heightened propensity of the compound in question to interact with cancer cells in comparison to normal cells. This finding indicates that the compound is more effective in inhibiting or killing cancer cells while having less toxicity or minimal effect on normal cells. The SI values of compounds **9a, 9c, 9d, 9e, 9b** and **9f** in PC-3 cells were calculated as 3.22, 2.51, 2.14, 1.98, 1.57 and 0.59, respectively, indicating high selectivity against prostate cancer cells, and the SI values of **9a, 9c, 9e, 9b, 9d** and **9f** in MCF-7 cells were 2.45, 1.68, 1.49, 1.29, 1.24 and 0.53, respectively, indicating that compounds **9a** and **9c** are selective against breast cancer cells.

2.3. Structure-Activity Relationship (SAR) Study

Considering the anticancer activity results, it was seen that most of the synthesized compounds have more selectivity index (SI) value than cisplatin. Only compound **9f** showed lower SI value than cisplatin. When the SI index of compounds **9a-f** were investigated, substitution of the coumarin ring was affected negatively SI index of compounds against both Prostate (PC-3) and Breast (MCF-7) cancer cell lines. Additionally, these substitutions resulted in increasing the interaction between synthesized compounds and healthy cells. This can be seen by looking at the CC_{50} values of compounds **9a-f** against Human Embryonic Kidney (HEK 293). The highest selectivity index against both prostate (PC-3) and breast (MCF-7) cancer cell lines was seen in compound **9a** with the value of 3.22 and 2.45, respectively. The second highest selectivity was seen in compound **9c** with the value of 2.51 and 1.68, respectively. The addition of chlorine group to coumarin ring in compound **9** resulted in the increase of selectivity index for both prostate (PC-3) and breast (MCF-7) cancer cell lines. It can be seen from compound **9b** (which has one Cl atom on coumarin ring) and **9e** (which has two Cl atoms on coumarin ring) (**Figure 4.**). Also, the addition of methoxy group to the coumarin ring in compound **9** decreased the SI index of both prostate (PC-3) and breast (MCF-7) cancer cell lines. It can be seen from the SI values of compound **9f** as 0.59 and 0.53, respectively.

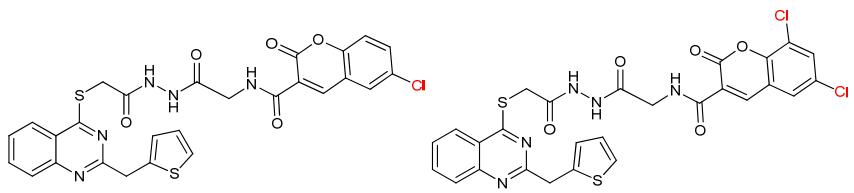

	9b	**9e**
SI value PC-3	1.57	1.29
SI value MCF-7	**1.98**	**1.49**

 doi:10.20944/preprints202508.1398.v1

Figure 4. SI value of compounds **9b** and **9e.**

According to anticancer activity results, compound **9f** showed the best activity against prostate and breast cancer cell lines with CC_{50} value of 14.7 ±1.4 and 16.5 ± 1.2 µg/L. When the activities of compounds **9a-f** were investigated, the addition of chlorine at the 5th position of the coumarin ring decreased the anticancer activities against both prostate and breast cancer cell lines. It can be seen from the activities of compounds **9a** and **9b (Figure 5.).**

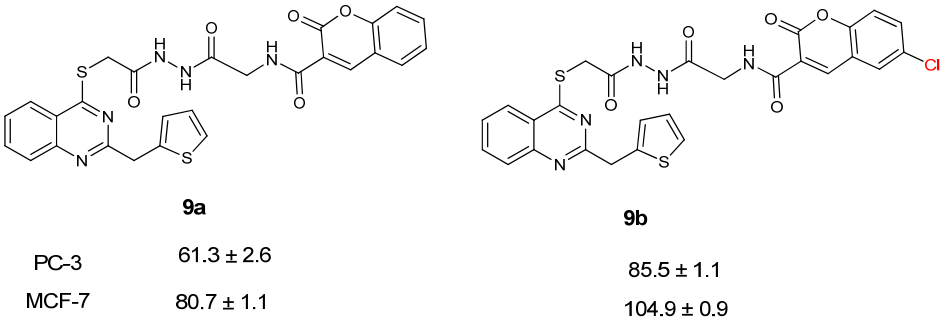

Figure 5. Anticancer activities of compounds **9a** and **9b** against PC-3 and MCF-7 cell lines.

When the activities of compounds **9b** and **9e** were compared, the addition of two chlorine at the 5th and 7th position of coumarin ring enhanced the anticancer activities against both prostate and breast cancer cell lines **(Figure 6.).**

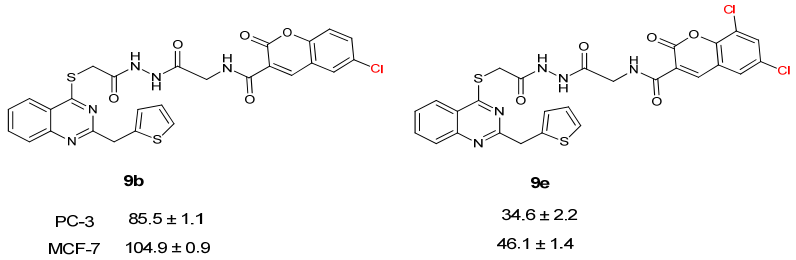

Figure 6. Anticancer activities of compounds **9b** and **9e** against PC-3 and MCF-7 cell lines.

When the activities of compounds **9a-f** were examined, it was observed that substitution at 7th position of the coumarin ring positively affected the anticancer activities against both prostate and breast cancer cell lines. Because of this reason, compounds **9f** and **9e** seem to be the most effective compounds against prostate and breast cancer cell lines **(Figure 7.).**

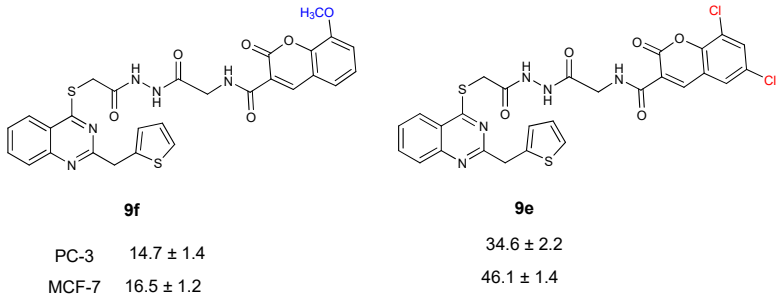

Figure 7. Anticancer activities of compounds **9f** and **9e** against PC-3 and MCF-7 cell lines.

 doi:10.20944/preprints202508.1398.v1

The summarized structure activity relationship (SAR) studies of the novel compounds **9a-f** is presented in **Figure 8.**

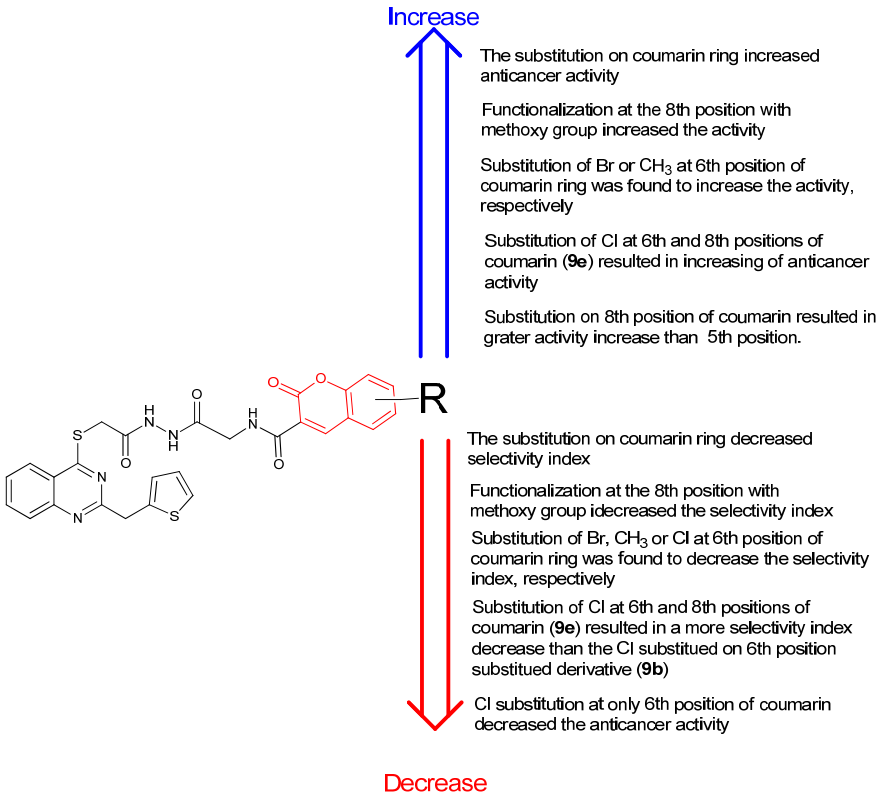

Figure 8. Summarized SAR of the synthesized compounds.

2.4. Molecular Docking Study

Molecular docking studies were utilized to understand the mechanism of anticancer activity of newly synthesized compounds, labeled **9a** through **9f** against three distinct cancer-related protein targets. The results of docking study were analyzed via binding affinity and interaction modes at the target proteins binding site. Our motivation in identifying target proteins was focused on elucidating the in vitro anticancer activity of the synthesized compounds. To this, kinesin related motor protein EG5, Human Ribonucleotide Reductase, and Topoisomerase II were selected due to their critical role in biological processes of cellular proliferation and DNA replication. EG5, a kinesin motor protein, is recognized for its essential role in mitotic spindle formation, a fundamental process in cell division [43]. Human Ribonucleotide Reductase is identified as a key enzyme in the synthesis pathway of deoxynucleotides, crucial building blocks for DNA [44]. Topoisomerase II is a well-known enzyme involved in managing DNA topology, facilitating processes like replication and transcription [45]. Due to their indispensable roles in the uncontrolled proliferation characteristic of tumor cells, these proteins have been widely investigated as therapeutic targets in the field of oncology. Inhibition of EG5 was known to induce mitotic arrest, while disruption of Human Ribonucleotide Reductase function was recognized to damage DNA synthesis in rapidly dividing cells. Similarly, the inhibition of Topoisomerase II activity was understood to lead to DNA damage and subsequent cell death in cancer cells.

The results of the docking simulation are presented in the **Table 2.** A comprehensive analysis of the generated scores revealed that compound **9f** consistently exhibited the most favorable predicted binding affinities across all investigated protein targets. Specifically, for the EG5 target, a binding score of -11.881 was recorded for compound **9f**. Against Human Ribonucleotide Reductase,

 doi:10.20944/preprints202508.1398.v1

compound **9f** achieved a score of -9.088. Furthermore, for Topoisomerase II, compound **9f** demonstrated a notably strong predicted affinity with a score of -12.694. In contrast to the vitro experiments, compound **9e** generally displayed the least favorable scores within the series, indicating a comparatively weaker predicted binding across the targets. Variations in the relative ranking of other compounds were observed depending on the specific protein target, suggesting diverse binding preferences within the series.

Table 2. Docking scores of newly synthesized compounds for selected targets.

	6G6Y	5TUS	3QX3
9a	-11.029	-7.99	-9.956
9b	-11.084	-7.133	-8.622
9c	-11.256	-6.627	-10.874
9d	-11.272	-8.368	-9.902
9e	-10.883	-7.603	-8.021
9f	-11.881	-9.088	-12.694

The interaction diagram showing the binding modes of Compound **9f** at the active site of kinesin-associated motor protein EG5 is given in **Figure 9-A,** and the main non-covalent interactions contributing to the stabilization of the ligand-protein complex were analyzed. Hydrogen bonds are formed between the NH group of the amide moiety of compound **9f** and Thr 222 and between the amide carbonyl and Trp 127. Water-bridged hydrogen bonding interactions were clearly observed in the binding pocket. It was observed that the Quinoxaline core of compound **9f** formed pi-pi stacking interactions with Trp 127. Hydrophobic interactions played an important role in the anchoring of compound **9f** to the binding site. The methoxy oxygen of the ligand is surrounded by the polar pocket, while the amid carbonyl, quinoxaline and thiophene ring are seen to be in the hydrophobic pocket. These interactions contribute to the stability of the ligand-protein complex and provide insights into the molecular basis of binding affinity.

A detailed two-dimensional interaction diagram depicting the binding pose (**Figure 9-B**) of compound **9f** within the active site of Human Ribonucleotide Reductase was thoroughly analyzed to elucidate the critical non-covalent interactions that contributed to the stability of the ligand-protein complex. Hydrogen bonding interactions were observed as significant contributors to the binding stability. Specifically, the carbonyl oxygen atom from the coumarin ring system of the ligand was found to engage in a hydrogen bond with the backbone NH group of Ser 606. Another hydrogen bond was formed between the methoxy oxygen of the coumarin moiety and the side chain OH group of Thr 607. Pi-pi stacking interactions were also identified as playing a role in the ligand's orientation within the active site. The quinoxaline ring of Compound 9f was observed to participate in a pi-pi stacking interaction with Phe 206. Hydrophobic interactions were extensively noted, indicating a substantial contribution to the overall binding. These interactions were represented by surrounding green envelopes and involved numerous residues within the active site, including Cys 218, Pro 203, Ala 201, Leu 446, Ala 447, and Ala 245. Portions of the ligand, specifically around the quinolone and coumarin systems, were also seen to be involved in polar contacts, indicated by light blue lines. These diverse non-covalent interactions collectively contributed to the strong predicted binding affinity of Compound **9f** to this vital enzyme, providing a molecular basis for its potential inhibitory activity.

The binding pose of Compound 9f within the active site of the Human Topoisomerase II enzyme, given in **Figure 9-C**, was analyzed to elucidate the specific ligand-protein and ligand-DNA interactions contributing to the stability of the ternary complex. Hydrogen bonding interactions were observed to be pivotal in anchoring compound **9f** within the active site. The nitrogen atom of the quinoxaline ring in compound **9f** was shown to form water-bridged hydrogen bonds with the backbone carbonyls of Ala 817. Direct hydrogen bonds were identified; one carbonyl oxygen from the coumarin-like ring system of the ligand was seen to interact with Pro 819 and DA F:12 DNA bases. Another carbonyl oxygen formed a hydrogen bond with Gln 778 and Ser 818. The amid carbonyl of

 doi:10.20944/preprints202508.1398.v1

the ligand also formed a direct hydrogen bonding interaction with the DA C:6 DNA bases. The NH group of compound **9f** also formed hydrogen bonding interactions with the DNA bases DG C:7. Hydrophobic interactions were extensively distributed throughout the binding pocket, contributing substantially to the overall complex stability. These multi-faceted interactions underscored the predicted stability of compound **9f** within the Topoisomerase II-DNA complex, providing a molecular foundation for its potent inhibitory activity against this vital anticancer target.

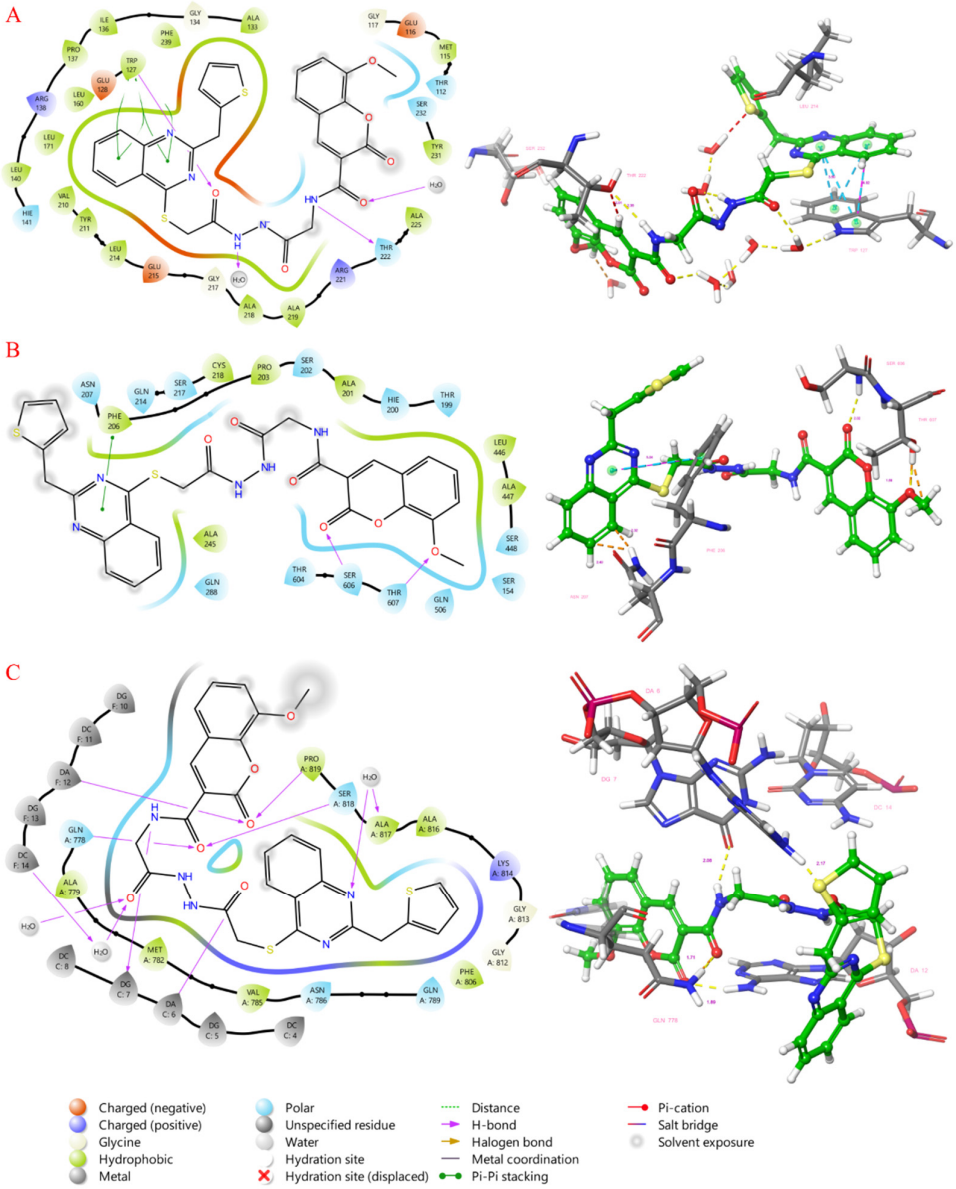

Figure 9. 2D and 3D ligand interaction diagram of compound **9f** at the binding site of EG5 (A), Human Ribonucleotide Reductase (B), and Topoisomerase II (C).

3. Materials and Methods

3.1. Experimental Synthesis

Synthesis of Compounds 9a–f

A mixture of compound 3 (3.30 g, 0.01 mol) and the corresponding compound 8a-f in dimethyl sulfoxide (DMSO) (25 mL) was subjected to heating in an oil bath for a period of 6 hours at 100 °C.

 doi:10.20944/preprints202508.1398.v1

Following the conclusion of the reaction (which was monitored by thin layer chromatography (TLC), ethyl acetate:hexane, 3:1), the mixture was poured into an ice-water mixture, yielding a yellow solid. The filtrate was subjected to a series of treatments, including filtration and washing with hot water and hot ethanol, respectively. The objective of the process was to obtain pure 9a-f.

2-Oxo-*N*-(2-oxo-2-{2-[(quinazolin-4-ylsulfanyl)acetyl]hydrazinyl}ethyl)-2*H*-chromene-3-carboxamide (9a). Yield 0.41 g, 73%; M.P. 255-256°C. FT-IR (KBR) ν_{max}, cm^{-1}: 3273, 3228, 3138 (NH), 1716, 1665, 1645, 1611 (C=O), 1566 (C=N). ^{1}H-NMR (400 MHz, DMSO-d_6), δ, ppm: 11.74 (s, 1H, NH), 9.83 (s, 1H, NH), 9.25 (s, 1H, NH), 8.94 (s, 1H, H-4 coumarin), 8.02-7.84 (m, 2H, ArH), 7.75 (t, 2H, *J*= 8 Hz, ArH), 7.52-7.45 (m, 2H, ArH), 7.28-6.98 (m, 5H, ArH), 4.51 (d, 2H, *J*= 4 Hz, SCH_2), 4.13 and 4.22 (s, 2H, NCH_2), 4.07 (s, 2H, CH_2). ^{13}C-NMR (100 MHz, DMSO-d_6), δ, ppm: 35.84 (CH_2), 42.05 (NCH_2), 51.06 (SCH_2), 116.51, 116.60, 118.75, 118.93, 125.63, 126.12, 127.25, 127.30, 130.85, 131.80, 137.19, 137.65, 144.07, 148.38, 154.43 (Ar-C), 157.24 (C=O), 160.90, 161.33 (C=O coumarin), 167.62 (C=N). LC-MS, *m*/*z*: 560.0 $[M+H]^+$, 582 $[M+Na]^+$. Calcd for $C_{27}H_{21}N_5O_5S_2$: elemental analysis: C, 57.95; H, 3.78; N, 12.51%; found: C, 57.87; H, 3.71; N, 12.43.

6-Bromo-2-oxo-*N*-(2-oxo-2-{2-[(quinazolin-4-ylsulfanyl)acetyl]hydrazinyl}ethyl)-2*H*-chromene-3-carboxamide (9b). Yield 0.47 g, 75%; M.P. 265-266°C. FT-IR (KBr) ν_{max}, cm^{-1}: 3258, 3225, 3200 (NH), 1742, 1662, 1641, 1612 (C=O), 1561 (C=N). ^{1}H-NMR (400 MHz, DMSO-d_6), δ, ppm: 11.78 (s, 1H, NH), 9.83 (s, 1H, NH), 9.25 (s, 1H, NH), 8.92 (s, 1H, H-4 coumarin), 8.17 (d, 1H, *J*= 4 Hz, ArH), 7.90 (d, 1H, *J*= 8 Hz, ArH), 7.56 (d, 1H, *J*= 4 Hz, ArH), 7.44 (d, 1H, *J*= 8 Hz, ArH), 7.23 (t, 1H, *J*= 12 Hz, ArH), 7.09 (d, 1H, *J*= 8 Hz, ArH), 7.07 (s, 1H, ArH), 6.97 (t, 1H, *J*= 8 Hz, ArH), 6.87 (t, 1H, *J*= 8 Hz, ArH), 6.83 (d, 1H, *J*= 4 Hz, ArH), 4.50 (d, 2H, *J*= 4 Hz, SCH_2), 4.18 (s, 2H, NCH_2), 4.08 (s, 2H, CH_2). ^{13}C-NMR (100 MHz, DMSO-d_6), δ, ppm: 35.84 (CH_2), 40.93 (NCH_2), 56.46 (SCH_2), 109.98, 115.79, 116.85, 117.12, 118.88, 119.84, 119.88, 120.74, 126.10, 127.24, 127.29, 132.68, 137.19, 137.66, 144.11, 145.17, 153.44 (Ar-C), 153.57 (C=N), 155.85, 157.24 (C=O), 161.03 (C=O coumarin), 167.54 (C=O). LC-MS, *m*/*z*: 639.3 $[M(Br^{79})\ (Br^{81})+H]^+$, 641.3 $[M(Br^{81})+H]^+$. Calcd for $C_{27}H_{20}BrN_5O_5S_2$: elemental analysis: C, 50.79; H, 3.16; N, 10.97%; found: C, 50.71; H, 3.10; N, 10.90.

6-Chloro-2-oxo-*N*-(2-oxo-2-{2-[(quinazolin-4-ylsulfanyl)acetyl]hydrazinyl}ethyl)-2*H*-chromene-3-carboxamide (9c). Yield 0.44 g (75%); M.P. 255-258°C. FT-IR (KBr) ν_{max}, cm^{-1}: 3315, 3234, 3140 (NH), 1724, 1645, 1612 (C=O), 1568 (C=N). ^{1}H-NMR (400 MHz, DMSO-d_6), δ, ppm: 11.78 (s, 1H, NH), 9.86 (s, 1H, NH), 9.34 (d, 1H, *J*= 4 Hz, NH), 8.92 (s, 1H, H-4 coumarin), 8.16 (t, 1H, *J*= 8 Hz, ArH), 7.90 (d, 1H, *J*= 8 Hz, ArH), 7.79 (d, 1H, *J*= 4 Hz, ArH), 7.58 (d, 1H, *J*= 4 Hz, ArH), 7.46 (d, 1H, *J*= 4 Hz, ArH), 7.32 (d, 1H, *J*= 4 Hz, ArH), 7.24 (t, 1H, *J*= 4 Hz, ArH), 7.10 (s, 1H, ArH), 6.98 (d, 1H, *J*= 4 Hz, ArH), 6.87 (t, 1H, *J*= 8 Hz, ArH) 4.52 (d, 2H, *J*= 8 Hz, SCH_2) 4.19 (s, 2H, NCH_2), 4.09 (s, 2H, CH_2). ^{13}C-NMR (100 MHz, DMSO-d_6), δ, ppm: 35.97 (CH_2), 42.12 (CH_2), 43.64 (CH_2), 118.62, 119.77, 120.40, 127.40, 129.32, 129.70, 134.02, 134.27, 147.76, 153.11 (Ar-C), 160.36, 160.50 161.14 (C=O), 161.64 (C=O coumarin), 167.86 (C=N). LC-MS, *m*/*z*: 635 $[M\ (Cl^{37})+K]^+$. Calcd for $C_{27}H_{20}ClN_5O_5S_2$: elemental analysis: C, 54.59; H, 3.39; N, 11.79%; found: C, 54.51; H, 3.32; N, 11.73.

6-Methyl-2-oxo-*N*-(2-oxo-2-{2-[(quinazolin-4-ylsulfanyl)acetyl]hydrazinyl}ethyl)-2*H*-chromene-3-carboxamide (9d). Yield 0.44 g (78%); M.P. 266-267°C. FT-IR (KBr) ν_{max}, cm^{-1}: 3308, 3141 (NH), 1721, 1708, 1644, 1614(C=O), 1571 (C=N). ^{1}H-NMR (400 MHz, DMSO-d_6), δ, ppm: 11.73 (s, 1H, NH), 10.50 and 9.82 (s, 1H, NH), 9.25 (d, 1H, *J*= 4 Hz, NH), 8.85 (s, 1H, H-4 coumarin), 7.87 (d, 1H, *J*= 8 Hz, ArH), 7.76 (s, 1H, ArH), 7.57-7.38 (m, 4H, ArH), 7.18-6.93 (m, 4H, ArH), 4.50 (d, 2H, *J*= 4 Hz, SCH_2), 4.22 and 4.12 (s, 2H, NCH_2), 4.06 (s 2H, CH_2), 2.37 (s, 3H, CH_3). ^{13}C-NMR (100 MHz, DMSO-d_6), δ, ppm: 20.69 (CH_3), 35.83 (CH_2), 42.03 (NCH_2), 43.46 (SCH_2), 116.35, 116.57, 116.96, 118.64, 123.51, 126.22, 127.33, 130.36, 131.89, 134.83, 135.58, 137.19, 137.65, 144.04, 148.30, 152.62 (Ar-C), 157.21, 160.11, 161.07 (C=O), 161.51 (C=O coumarin), 167.77 (C=N). TOF-MS, *m*/*z*: 574 $[M+H]^+$. Calcd for $C_{28}H_{23}N_5O_5S_2$: elemental analysis: C, 58.63; H, 4.04; N, 12.21%; found: C, 58.55; H, 3.96; N, 12.13.

6,8-Dichloro-2-oxo-*N*-(2-oxo-2-{2-[(quinazolin-4-ylsulfanyl)acetyl]hydrazinyl}ethyl)-2*H*-chromene-3-carboxamide (9e). Yield 0.51 g (81%); M.P. 280-282°C. FT-IR (KBr) ν_{max}, cm^{-1}: 3256 (NH), 1724, 1666, 1648, 1612 (C=O), 1561 (C=N). ^{1}H-NMR (400 MHz, DMSO-d_6), δ, ppm: 11.74 (s, 1H, NH), 10.48 and 9.82 (s, 1H, NH), 9.14 (s, 1H, NH), 8.88 (s, 1H, H-4 coumarin), 8.13-8.06 (m, 2H, ArH), 7.86

 doi:10.20944/preprints202508.1398.v1

(d, 1H, *J*= 8 Hz, ArH), 7.48-7.16 (m, 4H, ArH), 7.07 (s, 1H, ArH), 6.98-6.94 (m, 1H, ArH), 4.49 (d, 2H, *J*= 4 Hz, SCH_2), 4.15 (s, 2H, NCH_2), 4.06 (s, 2H, CH_2). ^{13}C-NMR (100 MHz, DMSO-d_6), δ, ppm: 36.75 (CH_2), 42.08 (NCH_2), 42.28 (SCH_2), 113.20, 117.16, 117.38, 118.76, 123.95, 123.98, 126.11, 131.31, 131.39, 136.85, 136.93, 142.20, 146.58, 150.44, 152.86 (Ar-C), 156.38, 161.67, 163.80 (C=O) 164.09 (C=O coumarin), 168.82 (C=N). LC-MS, *m/z*: 629 [M (Cl^{35})(Cl^{37})+H]$^+$. Calcd for $C_{27}H_{19}Cl_2N_5O_5S_2$: elemental analysis: C, 51.60; H, 3.05; N, 11.14%; found: C, 51.51; H, 2.98; N, 11.07.

8-Methoxy-2-oxo-*N*-(2-oxo-2-{2-[(quinazolin-4-ylsulfanyl)acetyl]hydrazinyl}ethyl)-2*H*-chromene-3-carboxamide (9f). Yield 0.45 g (76%); M.P. 284-285°C. FT-IR (KBr) ν_{max}, cm^{-1}: 3291 (NH), 1717, 1706, 1666, 1609 (C=O), 1524 (C=N).^{1}H-NMR (400 MHz, DMSO-d_6), δ, ppm: 11.73 (s, 1H, NH), 10.48 and 9.82 (s, 1H, NH), 9.25 (s, 1H, NH), 8.88 (s, 1H, H-4 coumarin), 7.87-7.86 (m, 1H, ArH), 7.51-7.25 (m, 5H, ArH), 7.18-7.07 (m, 2H, ArH), 6.93-6.80 (m, 2H, ArH), 4.50 (s, 2H, SCH_2), 4.22 and 4.21 (s, 2H, NCH_2), 4.06 (s, 2H, CH_2), 3.91 (s, 3H, OCH_3). ^{13}C-NMR (100 MHz, DMSO-d_6), δ, ppm: 35.83 (CH_2), 42.05 (NCH_2), 43.49 (NCH_2), 56.63 (OCH_3), 116.48, 116.83, 118.88, 119.40, 121.69, 125.50, 125.58, 126.09, 127.24, 131.76, 137.14, 137.64, 143.72, 144.06, 146.68, 148.55, 157.20 (Ar-C), 160,59, 161.28 (C=O), 167.61 (C=N). Calcd for $C_{28}H_{23}N_5O_6S_2$: elemental analysis: C, 57.03; H, 3.93; N, 11.88%; found: C, 56.93; H, 3.85; N, 11.82.

3.2. Anticancer Activity

The synthesized compounds, HEK-293 human embryonic kidney cell line, and cancer cell lines (MCF-7 breast and PC-3 prostate) were obtained from American Type Cell Culture Collection (ATCC, USA). The cancer and healthy cell lines were grown in a 5% CO_2 incubator, using Roswell Park Memorial Institute (RPMI) 1640 medium containing 10% fetal bovine serum and 1% penicillin. The activities of the synthesized compounds against HEK-293 human healthy embryonic kidney cell line and cancer cell lines (MCF-7 breast, PC-3 prostate) are given in **Table 1**. Cells were seeded in 96-well plates with 104 cells per well. The synthesized compounds were applied to the cells at increasing concentrations for 34, 48 and 72 hours. At the end of the incubation periods, 20 µL of MTT solution was added to each well and the plates were kept in a 37 °C incubator for another 4 hours. After the MTT solution was withdrawn from the wells, 200 µL of dimethyl sulfoxide was added to each well and the optical densities in the wells were measured in a spectrophotometer (Tecan Infinite 200 PRO, Switzerland) at a wavelength of 570 nm. Drug doses that killed 50% of the cells (CC50) were calculated using the CalcuSyn program. Graphpad prism 5.0, a commercial statistical program, was used for statistical analysis of the data obtained from the experimental and control groups. For the accuracy of the statistical data, each test was performed with 3 times. Results are given as mean ± standard deviation (SD). To determine the differences between the treatment groups and the control group, Student's t test was applied and $p<0.05$ was considered significant for all tests.

3.3. Molecular Docking Studies

Induced Fit Docking (IFD) protocol was performed to evaluate the binding affinities of compounds **9a-f** against three key protein targets of cancer therapy by using Schrodinger's molecular docking software [46,47] . The selected targets including Topoisomerase II with PDB ID 3QX3, Human Ribonucleotide Reductase with PDB ID 5TUS, and kinesin-associated motor protein EG5 with PDB ID 6G6Y were downloaded from Protein Data Bank (www.rcsb.org)[48–50]. The protein structures were prepared using the protein preparation wizard of Schrodinger's molecular docking software [51]. During the preparation, all water molecules except for 5 Å away from the binding site were removed, and missing hydrogens and side chains were added. The final structure of the protein was further optimized using PROPKA at physiological pH. The binding sites were selected in the region containing co-crystalized ligands. The grid box sizes were chosen to be the same as the co-crystallized molecules.

The synthesized molecules were built in Maestro Build Panel and prepared by LigPrep module by applying default parameters [52]. All conformations of the ligands were docked into the selected binding site using Induced Fit Docking (IFD) protocol combined with extra precision (XP) docking.

 doi:10.20944/preprints202508.1398.v1

4. Conclusion

In conclusion, we designed and synthesized six novel glycine conjugated hybrid compounds containing coumarin, thiophene and quinazoline moieties as potential prostate and breast cancer agents. Our findings demonstrated that compounds which have substitutions on coumarin ring have more activity than the compound which has no substitution (except for chlorine substitution of 6th position of coumarin ring) against both prostate and breast cancer cell lines. Among the synthesized compounds, **9f** (which has methoxy group on 8th position of coumarin ring) has the best activity against both prostate and breast cancer cell lines. The activity results of the compounds showed that substitution on 8th position on coumarin ring enhanced the anticancer activity as seen in compound **9f** and **9e**. When the selectivity index values of synthesized compounds against cancer cell lines were compared, substitution on coumarin ring resulted in decreasing selectivity index value. More substitution on 8th position on coumarin ring decreased the selectivity index value, as can be seen from the selectivity index value of **9e** and **9f**.

A direct correlation between the in silico docking results and the in vitro cytotoxicity was observed, particularly for compound **9f**. This compound consistently yielded the most favorable docking scores against EG5, Human Ribonucleotide Reductase, and Topoisomerase II, which aligned with its highest cytotoxic activity in the experimental assays. This suggested that the strong predicted binding affinities computationally determined for compound **9f** were translated into substantial cellular toxicity. The consistently strong predicted binding affinities of compound **9f** across EG5, Human Ribonucleotide Reductase, and Topoisomerase II strongly suggested its potential as a promising lead compound. These computational findings indicated that compound **9f** possessed the capacity to interact favorably with multiple proteins critically involved in cancer cell growth and survival. Such multi-target activity was considered a valuable attribute in the development of novel anticancer agents. However, these predictions necessitate rigorous experimental validation through in vitro and in vivo studies to confirm the actual binding affinities, potency, and selectivity, thereby advancing the potential for compound **9f** as a therapeutic candidate in cancer treatment.

The findings obtained from this study suggest that glycine conjugated quinazoline hybrids containing coumarin ring could possess potent anticancer properties. Another important point to consider is that changing the substitution on coumarin ring is one of the important factor affecting the anticancer activities. Consequently, these hybrid compounds could be considered further in the process of drug discovery and design, with the potential to develop new medications to treat cancer.

Author Contributions: Nedime Çalışkan: Project administration, Methodology, Funding acquisition, **Emre Menteşe:** Writing—review & editing, Project administration, Methodology, Funding acquisition, **Fatih Yılmaz:** Writing—review & editing, Writing—original draft, Formal analysis , Data curation, **Muhammed Süleyman İlhan:** Formal analysis, Data curation, **Mustafa Emirik:** Formal analysis, Data curation.

Funding: This studv has been supported by the Recep Tayyip Erdogan University Development Foundation (Grant number: 02025007021643).

Acknowledgments: The authors thank to the the Research Fund of Recep Tayyip Erdogan University (Project Number: FDK-2022-1367) for financial support.

Conflicts of Interest: The authors declare no conflicts of interest.

References

1. Bray, F.; Laversanne, M.; Sung, H.; Ferlay, J.; Siegel, R.L.; Soerjomataram, I.; Jemal, A. Global Cancer Statistics 2022: GLOBOCAN Estimates of Incidence and Mortality Worldwide for 36 Cancers in 185 Countries. *CA Cancer J Clin* **2024**, *74*, 229–263. doi:https://doi.org/10.3322/caac.21834.
2. Chen, S.; Cao, Z.; Prettner, K.; Kuhn, M.; Yang, J.; Jiao, L.; Wang, Z.; Li, W.; Geldsetzer, P.; Bärnighausen, T.; et al. Estimates and Projections of the Global Economic Cost of 29 Cancers in 204 Countries and Territories From 2020 to 2050. *JAMA Oncol* **2023**, *9*, 465–472. doi:10.1001/jamaoncol.2022.7826.

 doi:10.20944/preprints202508.1398.v1

3. Guida, F.; Kidman, R.; Ferlay, J.; Schüz, J.; Soerjomataram, I.; Kithaka, B.; Ginsburg, O.; Mailhot Vega, R.B.; Galukande, M.; Parham, G.; et al. Global and Regional Estimates of Orphans Attributed to Maternal Cancer Mortality in 2020. *Nat Med* **2022**, *28*, 2563–2572. doi:10.1038/s41591-022-02109-2.
4. James, N.D.; Tannock, I.; N'Dow, J.; Feng, F.; Gillessen, S.; Ali, S.A.; Trujillo, B.; Al-Lazikani, B.; Attard, G.; Bray, F.; et al. The Lancet Commission on Prostate Cancer: Planning for the Surge in Cases. *The Lancet* **2024**, *403*, 1683–1722. doi:10.1016/S0140-6736(24)00651-2.
5. Wang, L.; Lu, B.; He, M.; Wang, Y.; Wang, Z.; Du, L. Prostate Cancer Incidence and Mortality: Global Status and Temporal Trends in 89 Countries From 2000 to 2019. *Front Public Health* **2022**, *10*. doi:10.3389/fpubh.2022.811044.
6. Leong, S.P.; Witte, M.H. Cancer Metastasis through the Lymphatic versus Blood Vessels. *Clin Exp Metastasis* **2024**, *41*, 387–402. doi:10.1007/s10585-024-10288-0.
7. Jiang, X.; Wang, J.; Deng, X.; Xiong, F.; Zhang, S.; Gong, Z.; Li, X.; Cao, K.; Deng, H.; He, Y.; et al. The Role of Microenvironment in Tumor Angiogenesis. *Journal of Experimental & Clinical Cancer Research* **2020**, *39*, 204. doi:10.1186/s13046-020-01709-5.
8. Lugano, R.; Ramachandran, M.; Dimberg, A. Tumor Angiogenesis: Causes, Consequences, Challenges and Opportunities. *Cellular and Molecular Life Sciences* **2020**, *77*, 1745–1770. doi:10.1007/s00018-019-03351-7.
9. Saman, H.; Raza, S.S.; Uddin, S.; Rasul, K. Inducing Angiogenesis, a Key Step in Cancer Vascularization, and Treatment Approaches. *Cancers (Basel)* **2020**, *12*, 1172. doi:10.3390/cancers12051172.
10. Abood, R.G.; Abdulhussein, H.A.; Abbas, S.; Majed, A.A.; Al-Khafagi, A.A.; Adil, A.; Alsalim, T.A. Anti-Breast Cancer Potential of New Indole Derivatives: Synthesis, in-Silico Study, and Cytotoxicity Evaluation on MCF-7 Cells. *J Mol Struct* **2025**, *1326*, 141176. doi:10.1016/j.molstruc.2024.141176.
11. Miller, K.D.; Ortiz, A.P.; Pinheiro, P.S.; Bandi, P.; Minihan, A.; Fuchs, H.E.; Martinez Tyson, D.; Tortolero-Luna, G.; Fedewa, S.A.; Jemal, A.M.; et al. Cancer Statistics for the US Hispanic/Latino Population, 2021. *CA Cancer J Clin* **2021**, *71*, 466–487. doi:10.3322/caac.21695.
12. Chunarkar-Patil, P.; Kaleem, M.; Mishra, R.; Ray, S.; Ahmad, A.; Verma, D.; Bhayye, S.; Dubey, R.; Singh, H.; Kumar, S. Anticancer Drug Discovery Based on Natural Products: From Computational Approaches to Clinical Studies. *Biomedicines* **2024**, *12*, 201. doi:10.3390/biomedicines12010201.
13. Ongnok, B.; Chattipakorn, N.; Chattipakorn, S.C. Doxorubicin and Cisplatin Induced Cognitive Impairment: The Possible Mechanisms and Interventions. *Exp Neurol* **2020**, *324*, 113118. doi:10.1016/j.expneurol.2019.113118.
14. Soltan, O.M.; Shoman, M.E.; Abdel-Aziz, S.A.; Narumi, A.; Konno, H.; Abdel-Aziz, M. Molecular Hybrids: A Five-Year Survey on Structures of Multiple Targeted Hybrids of Protein Kinase Inhibitors for Cancer Therapy. *Eur J Med Chem* **2021**, *225*, 113768. doi:https://doi.org/10.1016/j.ejmech.2021.113768.
15. Sharifi-Rad, J.; Cruz-Martins, N.; López-Jornet, P.; Lopez, E.P.-F.; Harun, N.; Yeskaliyeva, B.; Beyatli, A.; Sytar, O.; Shaheen, S.; Sharopov, F.; et al. Natural Coumarins: Exploring the Pharmacological Complexity and Underlying Molecular Mechanisms. *Oxid Med Cell Longev* **2021**, *2021*. doi:10.1155/2021/6492346.
16. Sharma, M.; Vyas, V.K.; Bhatt, S.; Ghate, M.D. Therapeutic Potential of 4-Substituted Coumarins: A Conspectus. *European Journal of Medicinal Chemistry Reports* **2022**, *6*, 100086. doi:https://doi.org/10.1016/j.ejmcr.2022.100086.
17. An, G.; Morris, M.E. Chapter 3—Efflux Transporters in Cancer Resistance: Molecular and Functional Characterization of Breast Cancer Resistance Protein. In *Drug Efflux Pumps in Cancer Resistance Pathways: From Molecular Recognition and Characterization to Possible Inhibition Strategies in Chemotherapy*; Sosnik, A., Bendayan, R., Eds.; Academic Press, 2020; Vol. 7, pp. 67–96 ISBN 24683183.
18. Koley, M.; Han, J.; Soloshonok, V.A.; Mojumder, S.; Javahershenas, R.; Makarem, A. Latest Developments in Coumarin-Based Anticancer Agents: Mechanism of Action and Structure–Activity Relationship Studies. *RSC Med Chem* **2024**, *15*, 10–54. doi:10.1039/D3MD00511A.
19. Koley, M.; Han, J.; Soloshonok, V.A.; Mojumder, S.; Javahershenas, R.; Makarem, A. Latest Developments in Coumarin-Based Anticancer Agents: Mechanism of Action and Structure–Activity Relationship Studies. *RSC Med Chem* **2024**, *15*, 10–54. doi:10.1039/D3MD00511A.
20. Önder, A. Anticancer Activity of Natural Coumarins for Biological Targets. In; 2020; pp. 85–109.

 doi:10.20944/preprints202508.1398.v1

21. Gangopadhyay, A. Plant-Derived Natural Coumarins with Anticancer Potentials: Future and Challenges. *J Herb Med* **2023**, *42*, 100797. doi:10.1016/j.hermed.2023.100797.
22. Mofasseri, M.; Eini, E.; Mofasseri, S.; Hanifehpour, B.; Zanbili, F.; Poursattar Marjani, A. Anticancer Potential of Coumarins from the Ferulago Genus. *Results Chem* **2025**, *13*, 102033. doi:10.1016/j.rechem.2025.102033.
23. Kumari, P.; Kaur, M. Coumarin-Based Hybrid Compounds: A New Approach to Cancer Therapy. *J Mol Struct* **2025**, *1337*, 142149. doi:10.1016/j.molstruc.2025.142149.
24. Hricovíniová, J.; Hricovíniová, Z.; Kozics, K. Antioxidant, Cytotoxic, Genotoxic, and DNA-Protective Potential of 2,3-Substituted Quinazolinones: Structure—Activity Relationship Study. *Int J Mol Sci* **2021**, *22*, 610. doi:10.3390/ijms22020610.
25. Ghorab, M.M.; Abdel-Kader, M.S.; Alqahtani, A.S.; Soliman, A.M. Synthesis of Some Quinazolinones Inspired from the Natural Alkaloid L—Norephedrine as EGFR Inhibitors and Radiosensitizers. *J Enzyme Inhib Med Chem* **2021**, *36*, 218–238. doi:10.1080/14756366.2020.1854243.
26. Zayed, M.F. Medicinal Chemistry of Quinazolines as Anticancer Agents Targeting Tyrosine Kinases. *Sci Pharm* **2023**, *91*, 18. doi:10.3390/scipharm91020018.
27. Ling, Z.-N.; Jiang, Y.-F.; Ru, J.-N.; Lu, J.-H.; Ding, B.; Wu, J. Amino Acid Metabolism in Health and Disease. *Signal Transduct Target Ther* **2023**, *8*, 345. doi:10.1038/s41392-023-01569-3.
28. Jing, R.; Walczak, M.A. Peptide and Protein Desulfurization with Diboron Reagents. *Org Lett* **2024**, *26*, 2590–2595. doi:10.1021/acs.orglett.4c00609.
29. Liu, Y.-M.; Li, Y.; Liu, R.-F.; Xiao, J.; Zhou, B.-N.; Zhang, Q.-Z.; Song, J.-X. Synthesis, Characterization and Preliminary Biological Evaluation of Chrysin Amino Acid Derivatives That Induce Apoptosis and EGFR Downregulation. *J Asian Nat Prod Res* **2021**, *23*, 39–54. doi:10.1080/10286020.2019.1702028.
30. Butler, M.; van der Meer, L.T.; van Leeuwen, F.N. Amino Acid Depletion Therapies: Starving Cancer Cells to Death. *Trends in Endocrinology & Metabolism* **2021**, *32*, 367–381. doi:10.1016/j.tem.2021.03.003.
31. Naz, S.; Shah, F.A.; Nadeem, H.; Sarwar, S.; Tan, Z.; Imran, M.; Ali, T.; Li, J.B.; Li, S. Amino Acid Conjugates of Aminothiazole and Aminopyridine as Potential Anticancer Agents: Synthesis, Molecular Docking and in Vitro Evaluation. *Drug Des Devel Ther* **2021**, *Volume 15*, 1459–1476. doi:10.2147/DDDT.S297013.
32. Barbosa, F.; Araújo, J.; Gonçalves, V.M.F.; Palmeira, A.; Cunha, A.; Silva, P.M.A.; Fernandes, C.; Pinto, M.; Bousbaa, H.; Queirós, O.; et al. Evaluation of Antitumor Activity of Xanthones Conjugated with Amino Acids. *Int J Mol Sci* **2024**, *25*, 2121. doi:10.3390/ijms25042121.
33. Çalişkan, N.; Menteşe, E.; Yilmaz, F.; Ilhan, M.S. Synthesis and Anticancer Activities of Amide-Bridged Coumarin–Quinazolinone Hybrid Compounds. *Russian Journal of Organic Chemistry* **2024**, *60*, 918–926. doi:10.1134/S1070428024050142.
34. Menteşe, E.; Yılmaz, F.; Menteşe, M.; Beriş, F.Ş.; Emirik, M. Developing Effective Antimicrobial Agents: Synthesis and Molecular Docking Study of Ciprofloxacin-Benzimidazole Hybrids. *ChemistrySelect* **2024**, *9*, e202303173. doi:https://doi.org/10.1002/slct.202303173.
35. Yilmaz, F. Microwave-Assisted Synthesis and Investigation of Urease Inhibitory Activities of Some 1,2,4-Triazol-3-Ones Containing Salicyl and Isatin Moieties. *Russ J Gen Chem* **2024**, *94*, 2018–2022. doi:10.1134/S1070363224080152.
36. Güven, O.; Menteşe, E.; Bilgin Sökmen, B.; Emirik, M.; Akyüz, G. Benzimidazolone Conjugated Biscoumarins: Synthesis, Molecular Docking Studies, Urease, Lipase, and Acetylcholinesterase Inhibitory Activities. *J Mol Struct* **2025**, *1338*, 142362. doi:10.1016/j.molstruc.2025.142362.
37. Menteşe, E.; Güzel, Y.Ü.; Akyüz, G.; Karaali, N.Ü. Synthesis of Novel Quinazolinone-Triheterocyclic Hybrides as Dual Inhibition of Urease and Ache. *Journal of the Iranian Chemical Society* **2024**, *21*, 2425–2431. doi:10.1007/s13738-024-03080-0.
38. Yilmaz, F. Green Synthesis and Biological Evaluation of Some 1,2,4-Triazol-3-Ones. *Russian Journal of Organic Chemistry* **2024**, *60*, 513–521. doi:10.1134/S1070428024030205.
39. Akyüz, G.; Menteşe, E. Urease Inhibition Activity Studies of Novel Azabenzimidazole-Derived Compounds. *Russ J Gen Chem* **2024**, *94*, 2432–2437. doi:10.1134/S1070363224090214.
40. Akyüz, G. Synthesis and Urease Inhibition Activities of Some New Schiff Bases Benzimidazoles Containing Thiophene Ring. *Russ J Bioorg Chem* **2024**, *50*, 974–981. doi:10.1134/S1068162024030233.

 doi:10.20944/preprints202508.1398.v1

41. Çalışkan, N.; Akyüz, G.; Menteşe, E. A Facile Ultrasonic Synthesis Approach to 3-H-Quinazolinethione Derivatives and Their Urease Inhibition Studies. *Phosphorus Sulfur Silicon Relat Elem* **2024**, *199*, 293–298. doi:10.1080/10426507.2024.2333471.
42. Çalışkan, N.; Akyüz, G.; Menteşe, E. A Facile Ultrasonic Synthesis Approach to 3- *H* -Quinazolinethione Derivatives and Their Urease Inhibition Studies. *Phosphorus Sulfur Silicon Relat Elem* **2024**, *199*, 293–298. doi:10.1080/10426507.2024.2333471.
43. Castillo, A.; Justice, M.J. The Kinesin Related Motor Protein, Eg5, Is Essential for Maintenance of Pre-Implantation Embryogenesis. *Biochem Biophys Res Commun* **2007**, *357*, 694–699. doi:10.1016/j.bbrc.2007.04.021.
44. Aye, Y.; Li, M.; Long, M.J.C.; Weiss, R.S. Ribonucleotide Reductase and Cancer: Biological Mechanisms and Targeted Therapies. *Oncogene* **2015**, *34*, 2011–2021. doi:10.1038/onc.2014.155.
45. Nitiss, J.L. DNA Topoisomerase II and Its Growing Repertoire of Biological Functions. *Nat Rev Cancer* **2009**, *9*, 327–337. doi:10.1038/nrc2608.
46. Schrödinger Release 2018-4: Glide, Schrödinger, LLC, New York, NY, 2018.
47. Schrödinger Release 2018-4: Induced Fit Docking Protocol; Glide, Schrödinger, LLC, New York, NY, 2018; Prime, Schrödinger, LLC, New York, NY, 2018.
48. Ahmad, Md.F.; Alam, I.; Huff, S.E.; Pink, J.; Flanagan, S.A.; Shewach, D.; Misko, T.A.; Oleinick, N.L.; Harte, W.E.; Viswanathan, R.; et al. Potent Competitive Inhibition of Human Ribonucleotide Reductase by a Nonnucleoside Small Molecule. *Proceedings of the National Academy of Sciences* **2017**, *114*, 8241–8246. doi:10.1073/pnas.1620220114.
49. Talapatra, S.K.; Tham, C.L.; Guglielmi, P.; Cirilli, R.; Chandrasekaran, B.; Karpoormath, R.; Carradori, S.; Kozielski, F. Crystal Structure of the Eg5—K858 Complex and Implications for Structure-Based Design of Thiadiazole-Containing Inhibitors. *Eur J Med Chem* **2018**, *156*, 641–651. doi:10.1016/j.ejmech.2018.07.006.
50. Wu, C.-C.; Li, T.-K.; Farh, L.; Lin, L.-Y.; Lin, T.-S.; Yu, Y.-J.; Yen, T.-J.; Chiang, C.-W.; Chan, N.-L. Structural Basis of Type II Topoisomerase Inhibition by the Anticancer Drug Etoposide. *Science (1979)* **2011**, *333*, 459–462. doi:10.1126/science.1204117.
51. Schrödinger Release 2025-2: Protein Preparation Workflow; Epik, Schrödinger, LLC, New York, NY, 2024; Impact, Schrödinger, LLC, New York, NY; Prime, Schrödinger, LLC, New York, NY, 2025.
52. Schrödinger Release 2025-2: LigPrep, Schrödinger, LLC, New York, NY, 2025.